II acceptor adjacent to the proposed donor site, with the 4-OH end available for interaction with both E114 and C1 of the donor sugar. This position of lipid II is comparable to that of subsites +1 and +2 of the substrate in λL (*15*), with the prereaction GT_{51} substrates similar to the postreaction lysozyme products.

We propose that E114 is a Brønsted base and acts to directly abstract a proton from the 4-OH group of the lipid II acceptor. The deprotonated form of E114 may be stabilized by the adjacent R249 residue, strictly conserved as part of motif V. The proton abstraction step probably occurs concomitantly with the electrophilic migration of the donor C1 toward the acceptor 4-OH group (Fig. 4, A and B). In the moenomycin complex, the conserved E171 residue lies closer to the glyceric acid moiety than the phosphate-sugar linkage (the β phosphate in our substrate model), which in combination with pH activity profiles of the *E. coli* PBP1b enzyme (*16*) casts some doubt on whether E171 protonates the sugar-phosphate linkage to assist catalysis. Furthermore, mutants of this residue in *E. coli* PBP1b retain some residual activity, whereas those of our predicted Brønsted base, E114, do not (*9*). If E171 does not act to protonate the substrate, then we propose that it helps to coordinate the pyrophosphate group of the donor, either directly or via a divalent metal cation. The variable pH optima and divalent cation requirements of the GT_{51} family of enzymes (*17*–*19*) may result from varying local environments of the E171 residue. The S_N2-like reaction occurs between donor and acceptor, causing inversion at the donor C1 anomeric carbon and formation of the β1,4-linked product. The lipid-pyrophosphate leaving group of the donor is then free to diffuse away and be recycled in lipid II synthesis. We propose that translocation of the newly formed product to the donor site is assisted by a higher affinity for the pyrophosphate moiety in the donor site than in the acceptor site, with the conserved positively charged K155, K163, R167, and K168 residues located near the donor pyrophosphate region of the active site (Fig. 4C). This model is again reminiscent of the lysozyme active site, where the +1 and +2 subsites that match the modeled GT_{51} acceptor sugars possess the lowest substrate affinity of all the subsites. These two structures now provide a basis for addressing further questions about the mechanism of this important family of enzymes and for the design of new antibacterials. This work also opens the door for understanding structure and function relationships in other clinically important families of lipid-sugar GTs.

References and Notes

1. C. Goffin, J. M. Ghuysen, *Microbiol. Mol. Biol. Rev.* **62**, 1079 (1998).
2. T. D. Bugg *et al.*, *Biochemistry* **30**, 10408 (1991).
3. C. T. Walsh, *Science* **261**, 308 (1993).
4. R. C. Goldman, D. Gange, *Curr. Med. Chem.* **7**, 801 (2000).
5. P. Butaye, L. A. Devriese, F. Haesebrouck, *Antimicrob. Agents Chemother.* **45**, 1374 (2001).
6. Materials and methods are available as supporting material on *Science* Online.
7. C. Contreras-Martel *et al.*, *J. Mol. Biol.* **355**, 684 (2006).
8. Single-letter abbreviations for the amino acid residues are as follows: A, Ala; C, Cys; D, Asp; E, Glu; F, Phe; G, Gly; H, His; I, Ile; K, Lys; L, Leu; M, Met; N, Asn; P, Pro; Q, Gln; R, Arg; S, Ser; T, Thr; V, Val; W, Trp; and Y, Tyr.
9. M. Terrak *et al.*, *Mol. Microbiol.* **34**, 350 (1999).
10. L. Holm, C. Sander, *Nucleic Acids Res.* **27**, 244 (1999).
11. P. Welzel *et al.*, *Tetrahedron* **43**, 585 (1987).
12. J. Halliday, D. McKeveney, C. Muldoon, P. Rajaratnam, W. Meutermans, *Biochem. Pharmacol.* **71**, 957 (2006).
13. P. Welzel, *Chem. Rev.* **105**, 4610 (2005).
14. O. Ritzeler *et al.*, *Tetrahedron* **53**, 1675 (1997).
15. A. K. Leung, H. S. Duewel, J. F. Honek, A. M. Berghuis, *Biochemistry* **40**, 5665 (2001).
16. B. Schwartz *et al.*, *Biochemistry* **41**, 12552 (2002).
17. D. S. Barrett, L. Chen, N. K. Litterman, S. Walker, *Biochemistry* **43**, 12375 (2004).
18. D. Barrett *et al.*, *J. Bacteriol.* **187**, 2215 (2005).
19. M. Terrak, M. Nguyen-Disteche, *J. Bacteriol.* **188**, 2528 (2006).
20. C. Evrard, J. Fastrez, J. P. Declercq, *J. Mol. Biol.* **276**, 151 (1998).

21. We thank S. Withers for helpful mechanistic discussion. We are grateful for beam time and assistance at the Advanced Light Source. The atomic coordinates and structure factors of the apoenzyme and moenomycin complex have been deposited at the Protein Data Bank, with accession numbers 2OLU and 2OLV, respectively. Figures were prepared using PyMol (www.pymol.org). N.C.J.S. is a Howard Hughes Medical Institute (HHMI) international scholar, a Canadian Institute of Health Research (CIHR) scientist, and a Michael Smith Foundation for Health Research (MSFHR) senior scholar. A.L.L. is a MSFHR and CIHR fellow. This work was funded by CIHR and HHMI operating funds and infrastructure funds from the Canada Foundation of Innovation and MSFHR.

Supporting Online Material

www.sciencemag.org/cgi/content/full/315/5817/1402/DC1
Materials and Methods
SOM Text
Fig. S1
Table S1
References

23 October 2006; accepted 24 January 2007
10.1126/science.1136611

Dynamics of Replication-Independent Histone Turnover in Budding Yeast

Michael F. Dion,[1]*† Tommy Kaplan,[2,3]* Minkyu Kim,[4] Stephen Buratowski,[4] Nir Friedman,[2] Oliver J. Rando[1]†‡

Chromatin plays roles in processes governed by different time scales. To assay the dynamic behavior of chromatin in living cells, we used genomic tiling arrays to measure histone H3 turnover in G1-arrested *Saccharomyces cerevisiae* at single-nucleosome resolution over 4% of the genome, and at lower (~265 base pair) resolution over the entire genome. We find that nucleosomes at promoters are replaced more rapidly than at coding regions and that replacement rates over coding regions correlate with polymerase density. In addition, rapid histone turnover is found at known chromatin boundary elements. These results suggest that rapid histone turnover serves to functionally separate chromatin domains and prevent spread of histone states.

Characterizing the dynamic behavior of nucleosomes is key to understanding the diversity of biological roles of chromatin. Nucleosomes are evicted at many yeast promoters during gene activation (*1*–*4*) and are reassembled in trans upon repression (*5*). In *Drosophila*, active transcription leads to replacement of histone H3 by the variant isoform H3.3 (*6*, *7*), whereas in budding yeast (whose only H3 is an H3.3 homolog), passage of RNA polymerase II (Pol II) results in eviction of nucleosomes from some (*8*), but not all (*9*), coding regions. In contrast, studies in *Physarum polycephalum* suggest that H3 is not replaced during Pol II transcription (*10*). Furthermore, recent results in yeast suggest that H4 deposition is independent of transcription status (*11*). The disagreement between these studies leads us to map the locus-specific turnover rate of histone H3 at genomic scale so as to address two questions. First, is there evidence for general transcription-dependent H3 turnover? Second, are there additional mechanisms for histone turnover?

To measure turnover rates, we used yeast carrying constitutively expressed Myc-tagged histone H3, as well as an inducible Flag-tagged H3 (*5*) (fig. S1). Flag-H3 was induced in G1-arrested cells for varying amounts of time, chromatin was cross-linked and digested to mononucleosomes (*12*), and Myc- and Flag-tagged histones were immunoprecipitated sepa-

[1]Faculty of Arts and Sciences, Center for Systems Biology, Harvard University, Cambridge, MA 02138, USA. [2]School of Computer Science and Engineering, The Hebrew University, Jerusalem 91904, Israel. [3]Department of Molecular Genetics and Biotechnology, Faculty of Medicine, The Hebrew University, Jerusalem 91120, Israel. [4]Department of Biological Chemistry and Molecular Pharmacology, Harvard University, 240 Longwood Avenue, Boston, MA 02115, USA.

*These authors contributed equally to this work.
†Present address: Department of Biochemistry and Molecular Pharmacology, University of Massachusetts Medical School, Worcester, MA 01605, USA.
‡To whom correspondence should be addressed. E-mail: Oliver.Rando@umassmed.edu

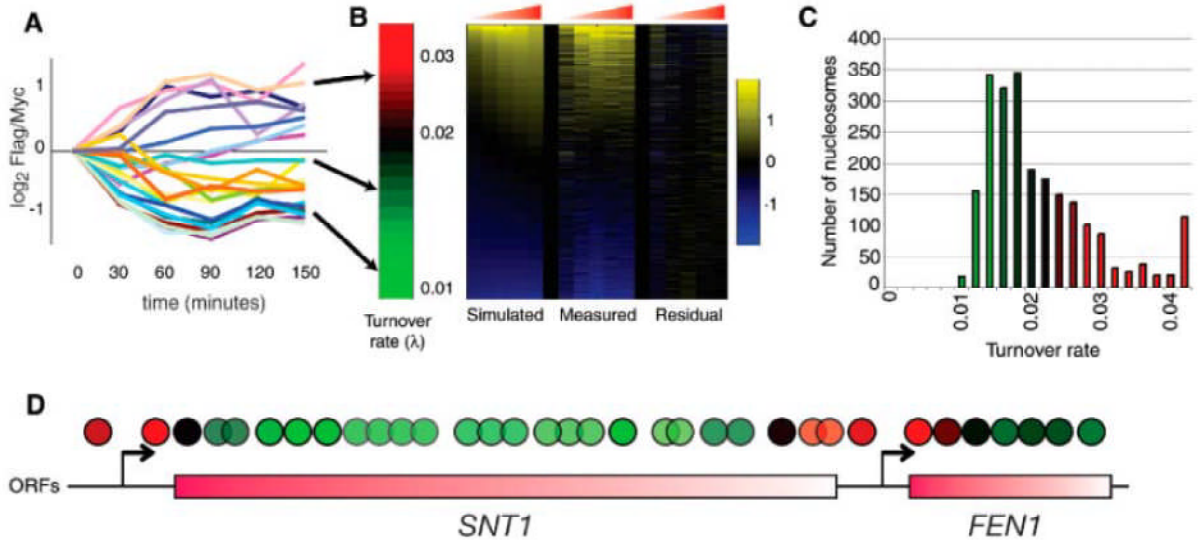

Fig. 1. Time courses of histone turnover in yeast. (**A**) H3 turnover for 23 adjacent nucleosomes in G1-arrested yeast cultures. Flag and Myc were immunoprecipitated at various time points after Flag-H3 induction (*x* axis), and Flag/Myc ratios (*y* axis) were measured by microarray. (**B**) A computational model reduces time course data to a single turnover parameter λ (frequency of histone turnover events, in units of min^{-1}), represented as the leftmost red-to-green color bar. Measured time-course data and data simulated using λ values are represented as blue-yellow heat maps (right). The minor differences (Residual) between measured and simulated data demonstrate that our model captures the majority of histone turnover dynamics during G1 arrest. (**C**) Distribution of turnover rates for nucleosomes in G1-arrested yeast. Binned turnover rates are color coded as in (B). (**D**) Sample genomic stretch, with nucleosomes (A) color coded by turnover rate.

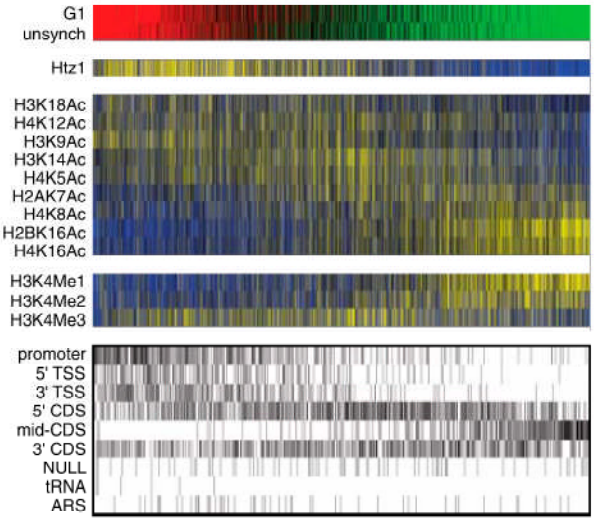

Fig. 2. Relation between histone modifications and H3 turnover, nucleosomes (columns) versus annotations (rows). Nucleosomes are ordered by turnover rate (red-to-green). Modification and Htz1 levels (*12*, *18*) are shown in yellow-to-blue heat maps, where yellow represents enrichment. The bottom panel shows genomic locations (*12*): 5′ and 3′ TSS refer to nucleosomes surrounding the transcriptional start site; promoter indicates other upstream probes. Protein-coding sequences are separated into 5′, middle, and 3′. Other annotations describe autonomously replicating sequences (ARSs), tRNA genes, and Null (any other intergenic region).

rately. Amplified DNAs were competitively hybridized to a 20–base pair (bp) resolution microarray covering 4% of the genome (*13*), yielding Flag/Myc ratios at each time point for each nucleosome on our array (Fig. 1A). We then estimated the turnover rate (number of H3 replacement events per unit of time) of each nucleosome using a simple analytical model that fits the experimental data with a small number of parameters (*14*, *15*) (Fig. 1B).

To test the validity of our results, we repeated the experiment in unsynchronized yeast (fig. S2), observing well-correlated but consistently faster turnover rates, as expected given global H3 deposition during genomic replication (Fig. 2 and fig. S3). We analyzed turnover rates in G1-arrested cells across the entire yeast genome using commercial microarrays with ~265-bp resolution (*16*, *17*) (fig. S4) and obtained a high correlation between rates from the two distinct measurement platforms (fig. S5). We also measured whole-genome histone occupancy (*1*, *3*) (*13*), finding that H3 replacement rates were weakly anticorrelated with H3 occupancy (fig. S6).

These results are consistent with those expected of H3 replacement from a free pool of H3 and demonstrate that we can recover semiquantitative turnover rates from time-course experiments. The time required for production of Flag-H3 (30 to 45 min) limits our ability to measure the rates of the hottest nucleosomes, which accumulate Flag-H3 before any protein can be detected by Western blot. We therefore caution against literal interpretation of turnover rates, because parameter choices (e.g., Flag-H3 degradation rate) affect absolute turnover rates; however, over a wide range of parameters, the ratio between estimated rates is robust. The resulting rate estimates span one to two orders of magnitude (depending on measurement platform) between "cold" nucleosomes that rarely turn over and hot ones whose replacement rate is faster than the time granularity of our experiment (Fig. 1C and Fig. 3B).

We compared high-resolution turnover rates to previously measured features of these nucleosomes (*12*, *17*, *18*) (Fig. 2 and fig. S7). Nucleosomes over protein-coding regions were coldest, whereas promoter nucleosomes were generally hot. Correspondingly, hot nucleosomes were depleted of the histone modifications that are "stereotypically" depleted surrounding the transcription start site (TSS) (*12*) and were conversely enriched for the histone H2A variant Htz1 (*16*, *18*).

These results are notable for two reasons. First, they suggest that replacement of TSS-adjacent nucleosomes with an appropriately modified nucleoplasmic pool could be partially responsible for promoter patterns of histone modification. Second, erasure of histone modifications due to rapid turnover would result in a steady-state picture of stereotyped promoter chromatin that does not capture transient states, potentially hiding any number of informative histone modification events.

Analysis of median replacement rates for various genomic loci confirmed that the most rapid turnover occurs over promoters, tRNA, and small nucleolar RNA genes (Fig. 3, A and B, and fig. S8). Most unexpected, given the dynamic H3.3 replacement over *Drosophila* genes (*7*, *19*), was the slow H3 turnover over protein-coding genes. Indeed, the coldest probes, mid–coding region probes, cover 28% of the genome yet account for only 10% of turnover. Despite the slower H3 turnover in coding regions, relative variation of turnover rates among coding regions might correlate with polymerase activity. For example, histone turnover over the alpha factor–inducible gene *FUS1* is more rapid in alpha factor–arrested cells than in unsynchronized cells (Fig. 3C and fig. S9). We therefore measured Pol II enrichment across the entire yeast genome, finding that polymerase enrichment over genes exhibited good correlation ($r^2 = 0.54$, $P < 6 \times 10^{-17}$)

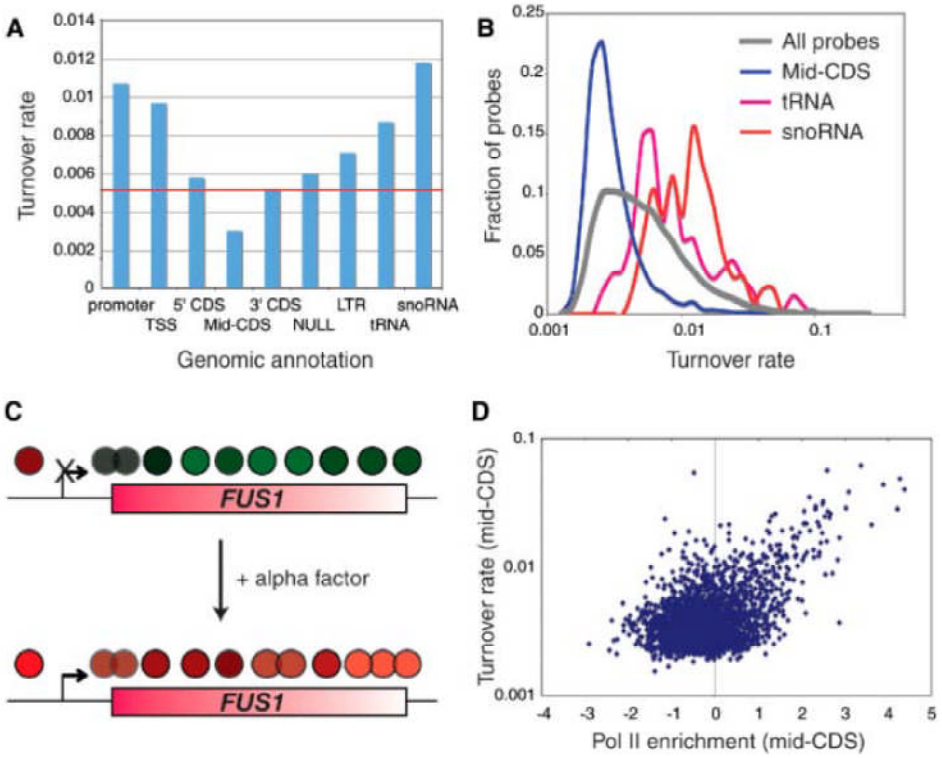

Fig. 3. Slow histone replacement over protein-coding genes. (**A**) Median turnover rates for genomic annotations (from whole-genome data). (**B**) Probe-level distributions of transcribed regions compared with the entire data set. *X* axis (logarithmic scale) shows turnover rate. *Y* axis shows fraction of probes within each rate bin. (**C**) *FUS1* coding region and associated nucleosomes, color coded according to turnover rates from high-resolution microarray experiments on unsynchronized yeast cultures (top), and G1-arrested cultures (bottom). (**D**) Scatter plot of coding region histone turnover (whole-genome data) versus $\log_2$ of Pol II enrichment.

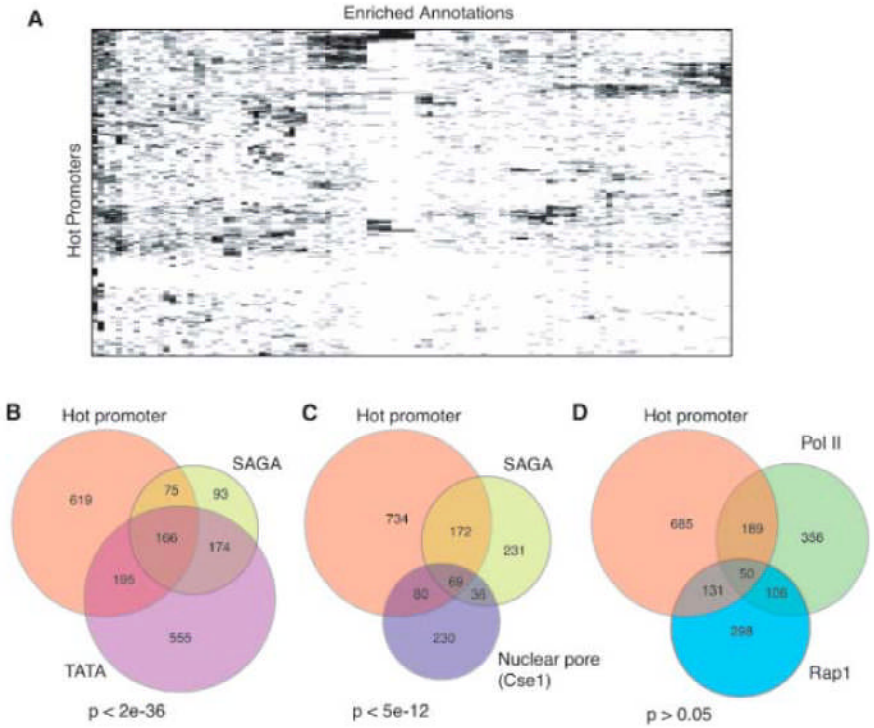

Fig. 4. Rapid turnover at promoters is associated with multiple partially overlapping features. (**A**) Hot promoters were tested for significantly enriched ($p < 10^{-7}$) annotations. Cluster diagram shows hot promoters as rows, annotations (table S6 and fig. S11) as columns. Black bars indicate positive annotations for a given promoter. (**B** to **D**) Overlap between hot promoters and pairs of enriched annotations. *P* value shows significance of overlap between pairs of annotations, given the extent of their overlap with hot promoters (hypergeometric distribution). SAGA-dominated genes are enriched for TATA-containing promoters (B) and are moderately correlated with Cse1-bound genes (C), whereas promoters with Rap1 sites are not enriched upstream of genes exhibiting high Pol II levels in our experiment (D).

with histone replacement rates (Fig. 3D). This is consistent with RNA polymerase passage evicting nucleosomes in some cases, although many highly transcribed genes (*RPL37B*, for example) exhibit low turnover rates.

Although polymerase passage and the resulting histone eviction represent a plausible first step for coding region histone turnover, they are unlikely to account for the bulk of histone replacement (Fig. 3A). Promoters of hot coding regions tend to be hot, but the converse is not true: Most hot promoters were adjacent to cold coding regions (e.g., Fig. 1D). Moreover, replacement rates at promoters were, unlike those at coding regions, poorly correlated with polymerase abundance, either at the promoter or over the coding region (fig. S10), making it unlikely that promoter turnover is solely a result of polymerase activity.

To systematically characterize promoter histone turnover, we tested the hottest subset of promoters for enrichment of published experimental and computational annotations (table S6). The hottest promoters include those carrying binding sites for a subset of transcription factors (such as Rap1, Reb1, Gcn4, and Adr1), those upstream of genes regulated by chromatin-modulating complexes (e.g., Ssn6/Tup1, Mediator, SAGA, Swi/Snf, and Sir), and those upstream of genes associated with nuclear pore components (e.g., Cse1, Mlp1, Nup116, and Nup2). Clustering hot promoters based on enriched annotations yielded independent clusters (Fig. 4A and fig. S11), such as a group of hot promoters associated with nuclear pore components (*20*). These separate clusters suggest that the many enrichments identified potentially

reflect multiple, partially overlapping mechanisms for rapid promoter turnover (Fig. 4, B to D). Some enrichments suggest clear hypotheses about the mechanism for rapid turnover (e.g., rapid histone replacement at Swi/snf-regulated promoters may well be a consequence of Swi/snf action), whereas other enrichments are less illuminating (e.g., what causes rapid replacement at nuclear pores?).

Many features of hot nucleosomes (including Htz1, tRNA genes, nuclear pore association, and Rap1 and Reb1 sites) are associated with boundaries that block heterochromatin spreading in yeast (*21*–*24*). How do boundaries block lateral spreading (*25*) of chromatin states? Suggested mechanisms include long gaps between nucleosomes, or recruited acetylases that compete with spreading deacetylation (*26*, *27*). The rapid H3 replacement at boundary-associated regions suggests an alternative hypothesis: that constant replacement of nucleosomes serves to erase a laterally spreading chromatin domain before it spreads any further (fig. S12). To investigate the role of Htz1 (whose role in boundary function is poorly understood) in histone replacement, we measured Flag-H3 incorporation in *htz1*Δ mutants, finding globally slowed H3 incorporation but few locus-specific effects (*14*). Further experiments will be required to untangle this relationship and to evaluate the role of rapid turnover at chromatin boundaries.

We have measured H3 replacement rates throughout the yeast genome, finding that nucleosomes over coding regions are replaced at high transcription rates, although most turnover occurs over promoters and small RNA genes. What function is served by histone replacement at promoters? Rapid turnover could transiently expose occluded transcription factor binding sites or it could ensure, by erasure of promoter chromatin marks, that transcriptional reinitiation occurs only in the continuing presence of an activating stimulus. Whatever the function, one important implication is that steady-state localization studies of histone marks could be confounded by dilution with histones carrying the average modification levels of the free histone pool, making dynamic or genetic studies key to deciphering any instructive roles of histone marks in transcriptional control. Finally, rapid turnover occurs at chromatin boundaries [see also (*28*)]. We propose that erasure of histone marks (or associated proteins) by rapid turnover delimits the spread of chromatin states. We further speculate that the widespread histone turnover at promoters throughout the compact yeast genome could serve, in a sense, to "expand" the genome by preventing chromatin states of adjacent genes from affecting each other.

References and Notes

1. B. E. Bernstein, C. L. Liu, E. L. Humphrey, E. O. Perlstein, S. L. Schreiber, *Genome Biol.* **5**, R62 (2004).
2. H. Boeger, J. Griesenbeck, J. S. Strattan, R. D. Kornberg, *Mol. Cell* **11**, 1587 (2003).
3. C. K. Lee, Y. Shibata, B. Rao, B. D. Strahl, J. D. Lieb, *Nat. Genet.* **36**, 900 (2004).
4. H. Reinke, W. Horz, *Mol. Cell* **11**, 1599 (2003).
5. U. J. Schermer, P. Korber, W. Horz, *Mol. Cell* **19**, 279 (2005).
6. K. Ahmad, S. Henikoff, *Mol. Cell* **9**, 1191 (2002).
7. Y. Mito, J. G. Henikoff, S. Henikoff, *Nat. Genet.* **37**, 1090 (2005).
8. M. A. Schwabish, K. Struhl, *Mol. Cell. Biol.* **24**, 10111 (2004).
9. A. Kristjuhan, J. Q. Svejstrup, *EMBO J.* **23**, 4243 (2004).
10. C. Thiriet, J. J. Hayes, *Genes Dev.* **19**, 677 (2005).
11. J. Linger, J. K. Tyler, *Eukaryot. Cell* **5**, 1780 (2006).
12. C. L. Liu *et al.*, *PLoS Biol.* **3**, e328 (2005).
13. G. C. Yuan *et al.*, *Science* **309**, 626 (2005).
14. Materials and methods are available as supporting material on *Science* Online.
15. Genomic turnover rates can be viewed at the University of California, Santa Cruz, Genome Browser on *S. cerevisiae*; http://compbio.cs.huji.ac.il/Turnover
16. B. Guillemette *et al.*, *PLoS Biol.* **3**, e384 (2005).
17. D. K. Pokholok *et al.*, *Cell* **122**, 517 (2005).
18. R. M. Raisner *et al.*, *Cell* **123**, 233 (2005).
19. K. Ahmad, S. Henikoff, *Proc. Natl. Acad. Sci. U.S.A.* **99**, (Suppl. 4), 16477 (2002).
20. J. M. Casolari *et al.*, *Cell* **117**, 427 (2004).
21. D. Donze, C. R. Adams, J. Rine, R. T. Kamakaka, *Genes Dev.* **13**, 698 (1999).
22. K. Ishii, G. Arib, C. Lin, G. Van Houwe, U. K. Laemmli, *Cell* **109**, 551 (2002).
23. M. D. Meneghini, M. Wu, H. D. Madhani, *Cell* **112**, 725 (2003).
24. Q. Yu *et al.*, *Nucleic Acids Res.* **31**, 1224 (2003).
25. L. N. Rusche, A. L. Kirchmaier, J. Rine, *Annu. Rev. Biochem.* **72**, 481 (2003).
26. X. Bi, J. R. Broach, *Curr. Opin. Genet. Dev.* **11**, 199 (2001).
27. Y. H. Chiu, Q. Yu, J. J. Sandmeier, X. Bi, *Genetics* **165**, 115 (2003).
28. Y. Mito *et al.*, *Science* **315**, 1408 (2007).

29. We thank K. Ahmad, N. Francis, A. Gasch, N. Habib, A. Jaimovich, R. Kupferman, H. Margalit, and I. Wapinski for critical reading of the manuscript. We thank P. Korber for the generous gift of the USY6 strain. O.J.R. is supported in part by a Career Award in Biomedical Sciences from the Burroughs Wellcome Fund. This research was supported by grants to O.J.R., S.B., and N.F. from the National Institute of General Medical Sciences, NIH; to O.J.R. from the Human Frontiers Science Program; and to N.F. from the Israeli Science Foundation. O.J.R. designed the experiments, and M.F.D. carried them out. S.B. designed, and M.K. carried out, Pol II chromatin immunoprecipitation. T.K., N.F., and O.J.R. analyzed the data. O.J.R. and N.F. wrote the paper.

Supporting Online Material

www.sciencemag.org/cgi/content/full/315/5817/1405/DC1
Materials and Methods
Figs. S1 to S18
Tables S1 to S6

18 August 2006; accepted 6 February 2007
10.1126/science.1134053

Histone Replacement Marks the Boundaries of cis-Regulatory Domains

Yoshiko Mito,[1,2] Jorja G. Henikoff,[1] Steven Henikoff[1,3]*

Cellular memory is maintained at homeotic genes by cis-regulatory elements whose mechanism of action is unknown. We have examined chromatin at *Drosophila* homeotic gene clusters by measuring, at high resolution, levels of histone replacement and nucleosome occupancy. Homeotic gene clusters display conspicuous peaks of histone replacement at boundaries of cis-regulatory domains superimposed over broad regions of low replacement. Peaks of histone replacement closely correspond to nuclease-hypersensitive sites, binding sites for Polycomb and trithorax group proteins, and sites of nucleosome depletion. Our results suggest the existence of a continuous process that disrupts nucleosomes and maintains accessibility of cis-regulatory elements.

Chromatin can be differentiated by the replication-independent replacement of one histone variant with another (*1*). For example, histone H3.3 is deposited throughout the cell cycle, replacing H3 that is deposited during replication (*2*–*4*). Unlike replication-coupled assembly of H3, which occurs in gaps between old nucleosomes on daughter helices, the insertion of H3.3 is preceded by disruption of preexisting histones during transcription and other active processes (*3*, *5*). We have previously shown that H3.3 replacement profiles resemble those for RNA polymerase II (*2*), which suggests that gradual replacement of H3.3 occurs in the wake of transiting polymerase to repair disrupted chromatin (*1*). Here, we ask whether histone replacement and nucleosome occupancy are also distinctive at cis-regulatory elements.

Log-phase *Drosophila melanogaster* S2 cells were induced to produce biotin-tagged H3.3 for two or three cell cycles (*2*). DNA was extracted from streptavidin pull-down assay and input material, labeled with Cy3 and Cy5 dyes, and cohybridized to microarrays. To provide a standard, we profiled biotin-tagged H3-containing chromatin in parallel. Analysis of H3.3/H3 levels over the entire *3*R chromosome arm revealed that the ~350-kb bithorax complex (BX-C) region displays the lowest H3.3/H3 ratio of any region of comparable size on *3*R, and the Antennapedia

[1]Basic Sciences Division, Fred Hutchinson Cancer Research Center, 1100 Fairview Avenue North, Seattle, WA 98109, USA. [2]Molecular and Cellular Biology Program, University of Washington, Seattle, WA 98195, USA. [3]Howard Hughes Medical Institute, Fred Hutchinson Cancer Research Center, Seattle, WA 98109, USA.

*To whom correspondence should be addressed. E-mail: steveh@fhcrc.org